JOURNAL OF MATERIALS SCIENCE 18 (1983) 173–178

X-ray photoelectron spectroscopic studies of surface oxidation of metallic glasses

P. SEN, A. SRINIVASAN, M. S. HEDGE, C. N. R. RAO
Solid State and Structural Chemistry Unit, Indian Institute of Science, Bangalore-560012, India

Surface oxidation of the metallic glass $Fe_{40}Ni_{38}Mo_4B_{18}$ has been studied by X-ray photoelectron spectroscopy. The oxidation behaviour of the metallic glass has been compared with a crystallized sample of the same composition. A similar study has been carried out on the metallic glass $Ni_{76}Si_{12}B_{12}$, which shows the importance of chemical composition in determining the surface oxidation behaviour of these alloys.

1. Introduction

X-ray photoelectron spectroscopy (XPS) has been extensively employed to study surface oxidation of metals [1–3]. This is an extremely good surface technique, and can distinctly identify different species present on a metal surface. The different metal oxides formed on a metal surface can be identified by the shift of metal core level binding energies, and the thickness of oxide layers on the surface can be obtained from the decrease in the intensity of metal core level peaks. We considered it interesting to investigate the surface oxidation of rapidly quenched metallic glasses by this technique since there is little or no information on this aspect of these novel materials [4]. It has, however, been known that some of the metallic glasses are more resistant to corrosion than crystalline alloys [5, 6]. Therefore, we have compared the surface oxidation behaviour of two metallic glasses with that of crystallized samples of the same compositions. The metallic glasses investigated are $Fe_{40}Ni_{38}Mo_4B_{18}$ and $Ni_{76}Si_{12}B_{12}$.

2. Experimental details

The metallic glasses, $Fe_{40}Ni_{38}Mo_4B_{18}$ (Allied 2826 MB) and $Ni_{76}Si_{12}B_{12}$ (Vacuum Sehmelzie, Hanau) were obtained in the form of ribbons. X-ray photoelectron spectra of these glasses were recorded using an ESCA-3 Mark II spectrometer of V.G. Scientific Limited, UK, fitted with a sample preparation chamber. The samples were etched with argon ions to obtain surfaces devoid of oxygen. The argon ion beam was defocused to avoid local heating of the sample surface. Oxygen exposures in Langmuir units, L (1 L = 10^{-6} torr sec), were given in the sample preparation chamber and the spectra recorded immediately under an operating vacuum of 10^{-10} torr [7, 8]. The metallic glasses were heated to about 820 K for 30 min in the sample preparation chamber under ultra-high velocity to obtain the crystallized samples.

Depth profile composition analysis of both the amorphous and crystalline samples of the alloys was carried out by measuring the core level peak intensities in XPS after successive argon ion etchings (4 kV; 50 μA). In the case of $Fe_{40}Ni_{38}Mo_4B_{18}$, we found a greater preponderance of iron and nickel relative to molybdenum or boron on the surface of the crystallized sample. Similarly, the Ni concentration was higher in the crystallized sample of $Ni_{76}Si_{12}B_{12}$.

3. Results and discussion

3.1. $Fe_{40}Ni_{38}Mo_4B_{18}$

Typical spectra in the Fe($2p_{3/2}$) and B(1s) regions of the alloy $Fe_{40}Ni_{38}Mo_4B_{18}$ are shown in Figs 1 and 2 to illustrate the nature of changes occurring on exposure to oxygen. In the low oxygen exposure range (~ 10 L), metal core level intensities (XPS peak heights) show a slight increase with exposure. The increase in metal substrate peak intensity is appreciable up to 7 L, decreasing drastically thereafter. Boron, however, behaves differently; there is

0022–2461/83/010173–06$03.22/0

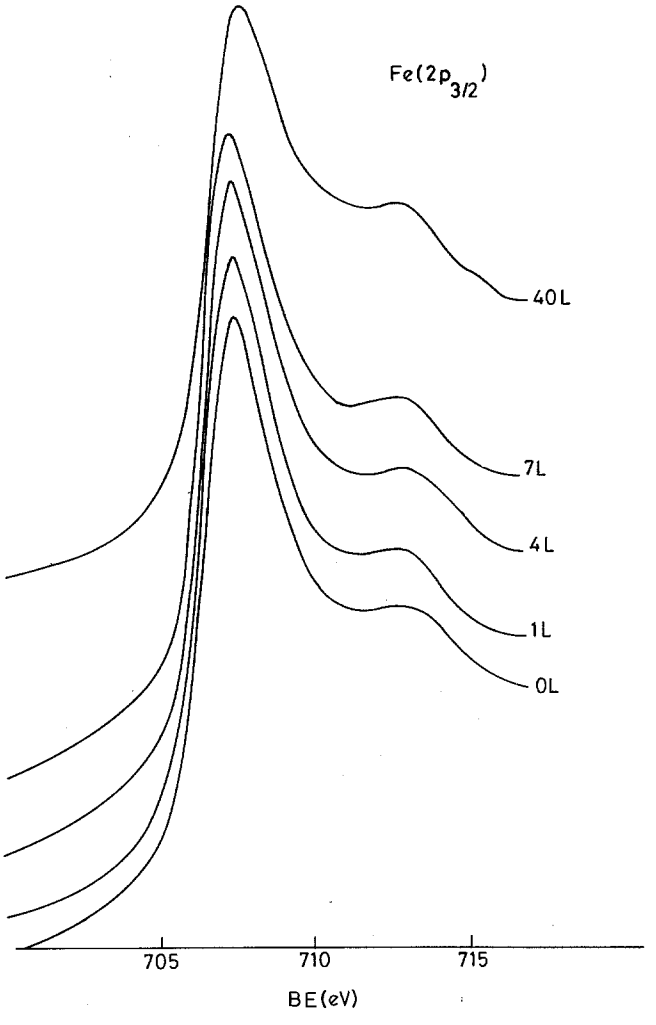

Figure 1 Variation in the $Fe(2p_{3/2})$ signal of $Fe_{40}Ni_{38}Mo_4B_{18}$ with oxygen exposure showing the initial oxidation stages.

no sudden increase in B(1s) peak intensity and the decrease in intensity at moderate exposures in the partially crystalline state is not as drastic as in the amorphous state. To illustrate this process in the region prior to oxide layer formation, the peak intensities of $Fe(2p_{3/2})$ and $Ni(2p_{3/2})$ were plotted with respect to B(1s) and $Mo(3d_{5/2})$, in Figs 3 and 4. The rise in the core level intensities of Fe and Ni with respect to boron can be seen in Fig. 3a and b. Although the intensity increases in both the amorphous and crystalline samples, it is more pronounced in the latter. Fig. 4a shows the changes in iron and molybdenum concentrations to be quite similar; nickel concentration, on the other hand, changes identically with molybdenum in the metallic glass, but shows an increase in the crystallized state at low to moderate exposure.

According to the model of Fehlner and Mott for the oxidation of thin films [9], a strong field is set up across an oxide film, evidence for which is

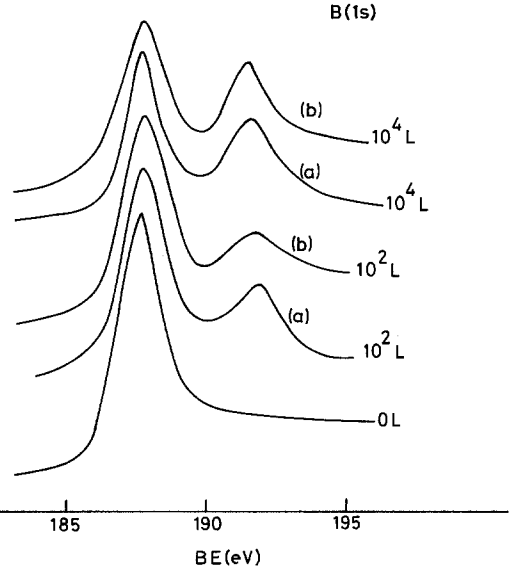

Figure 2 Variation in the B(1s) signal of $Fe_{40}Ni_{38}Mo_4B_{18}$ with oxygen exposure: (a) metallic glass; (b) crystallized sample.

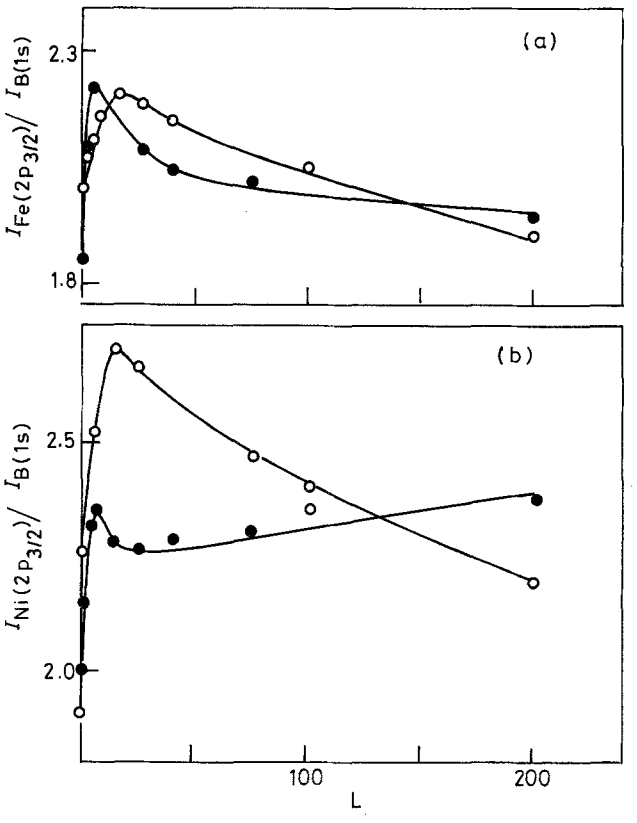

Figure 3 Variation in the intensities of $Fe(2p_{3/2})$ and $Ni(2p_{3/2})$ peaks of $Fe_{40}Ni_{38}Mo_4B_{18}$ relative to the B(1s) peak with oxygen exposure: •, metallic glass; ○, crystallized sample.

given by surface potential measurements. Oxygen ions move into the bulk, displacing the metal to the surface by place exchange due to an image force being set up. Place exchange becomes difficult after the formation of a monolayer of the oxide when oxidation at the surface is favoured. The increase in Ni concentration is more pronounced in the crystallized sample indicating that crystallization facilitates the drift of ions; Fe and Mo do not show this effect, possibly because surface oxidation is more rapid in these cases. Boron, which has a greater relative abundance in

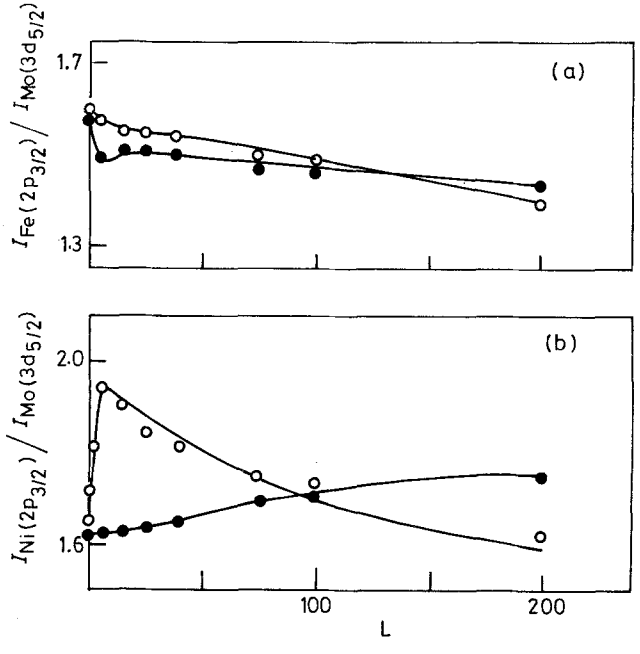

Figure 4 Variation in the intensities of $Fe(2p_{3/2})$ and $Ni(2p_{3/2})$ peaks of $Fe_{40}Ni_{38}Mo_4B_{18}$ relative to the $Mo(3d_{5/2})$ peak with oxygen exposure: •, metallic glass; ○, crystallized sample.

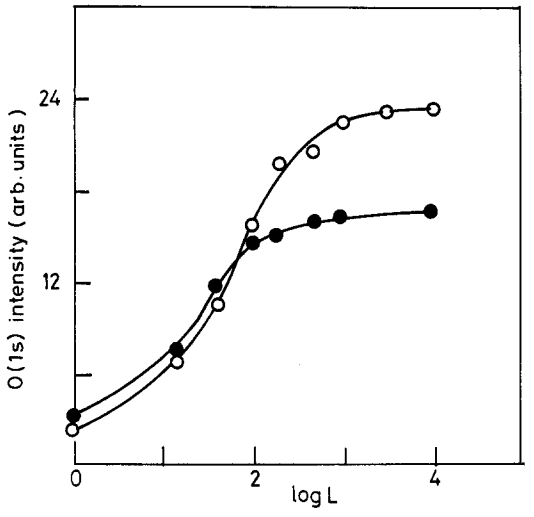

Figure 5 Total oxygen uptake on the surface of the metallic glass (•) and the crystallized sample (○) of $Fe_{40}Ni_{38}Mo_4B_{18}$ at different oxygen exposures.

the metallic glass, shows a more rapid decrease in intensity in this state compared to the crystallized state of the sample.

Oxygen uptake on the surface of the alloy is shown in Fig. 5 in terms of the variation of the O(1s) intensity with oxygen exposure. The total oxygen uptake is significantly larger on the surface of the crystallized sample compared to that of the metallic glass. The binding energy of the core level of oxygen (1s) is an indicator of the state of binding of oxygen to a surface. The 1 s binding energy decreases to a lower value as charge transfer takes place from the metal site to the ligand site on oxide formation, filling up the oxygen valence levels [10]. The O(1s) binding energy in the case of the metallic glass was ~ 530 eV at low oxygen exposures (1 L O_2) suggesting that oxygen dissociated on the surface tends to form an oxide layer. In the crystalline sample, on the other hand, the binding energy (531.5 eV) suggest the presence of dissociated oxygen which has still not formed an oxide layer. On further exposure to O_2 the O(1s) binding energy shifts to 529.8 eV indicating the formation of oxide layers.

We have attempted to make a quantitative comparison of the oxidation behaviour of the metallic glass with that of the crystallized sample, by calculating the number of oxide layers of Fe, Ni, Mo and B formed on the surface as a function of oxygen exposure. The number of oxide layers was calculated by making use of the decrease in the metal core level intensities and fitting them to the formula, $I(x) = I_0 \exp(-x/\lambda)$, where $I(x)$ is the intensity of the metal core level peak when the

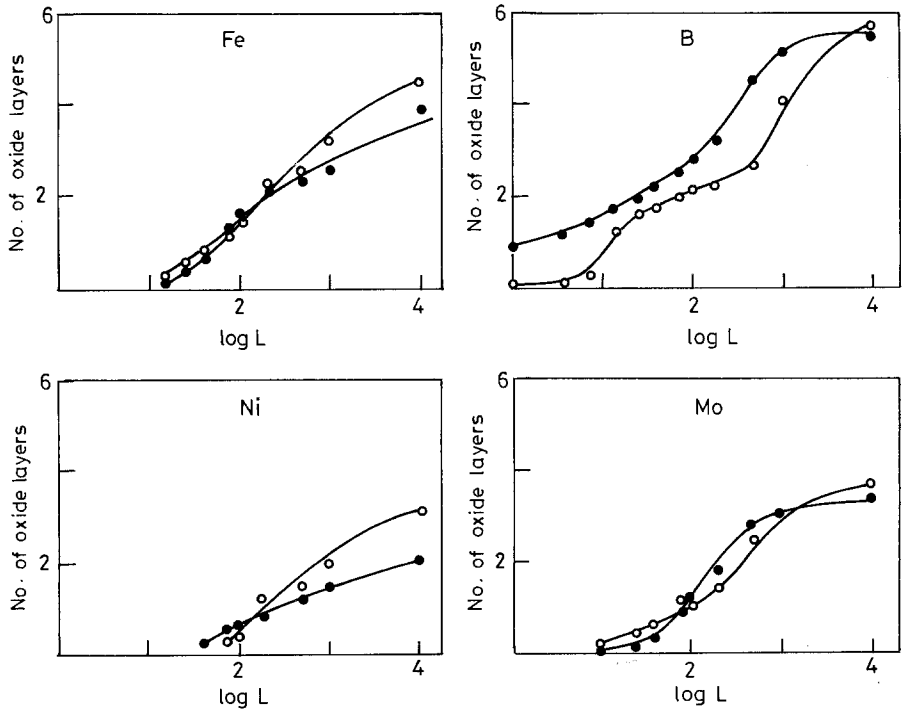

Figure 6 Number of oxide layers of Fe, Ni, Mo and B formed in the surface oxidation of $Fe_{40}Ni_{38}Mo_4B_{18}$: •, metallic glass; ○, crystallized sample.

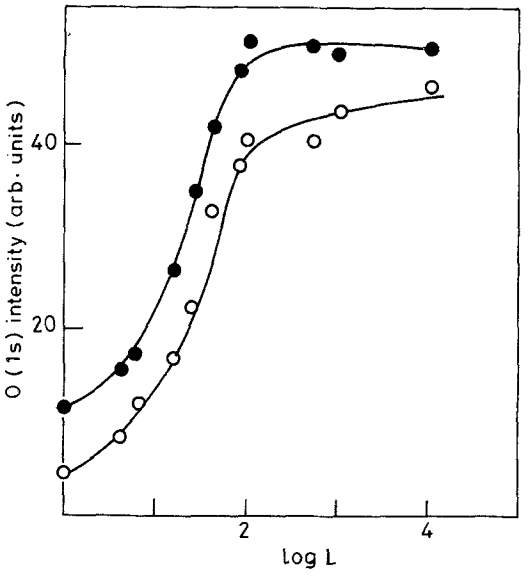

Figure 7 Total oxygen uptake on the surface of the metallic glass (•) and the crystallized sample (○) of $Ni_{76}Si_{12}B_{12}$ at different oxygen exposures.

coverage is x, and λ is the mean free path. The values of λ were taken to be 7, 6, 9.5 and 9.0 monolayers for $Fe(2p_{3/2})$, $Ni(2p_{3/2})$, B(1s) and $Mo(3d_{5/2})$, respectively. Peak heights, as well as the areas under the peaks, were employed as measures of intensity [11].

The number of oxide layers of the different elements in the amorphous as well as the crystalline forms of the alloy have been plotted against exposure (log L) in Fig. 6. Initially, boron forms a larger number of oxide layers in the metallic glass than in the crystallized sample; the difference is marginal in the case of molybdenum. Iron and nickel, on the other hand, show a larger number of oxide layers in the crystalline sample compared to the metallic glass. It is noteworthy that surface composition analysis, mentioned earlier, indicated an enrichment of the surface in iron and nickel in the crystallized sample. From the behaviour of the different elements in the alloy towards surface oxidation, it appears that the metalloid element, boron, forms a protective oxide layer more easily on the metallic glass, thereby decreasing the oxidation of iron and nickel. We also see from Fig. 6 that boron shows two distinct stages of oxidation in the crystallized sample as compared to iron, nickel or molybdenum. This may be taken to indicate that boron is oxidized in two different sites. Such preferential oxidation at interior defect sites and grain boundaries is indeed known to occur. Evidence has been presented [12, 13] for the formation of a protective oxide layer of the metalloid Si, in the oxidation of $Pd_{81}Si_{19}$.

3.2. $Ni_{76}Si_{12}B_{12}$

Unlike the $Fe_{40}Ni_{38}Mo_4B_{18}$ alloy, we find that in the $Ni_{76}Si_{12}B_{12}$ alloy, the total oxygen uptake is much greater on the surface of the metallic glass than on the crystallized sample (Fig. 7) though the uptake behaviour is essentially the same. The oxygen uptake here is essentially governed by the oxidation of the metalloid elements B and Si, hence showing similar trends; the extent of Ni oxidation being the same in both the states. On the other hand, in $Fe_{40}Ni_{38}Mo_4B_{18}$, the metals, iron and nickel are more oxidized in

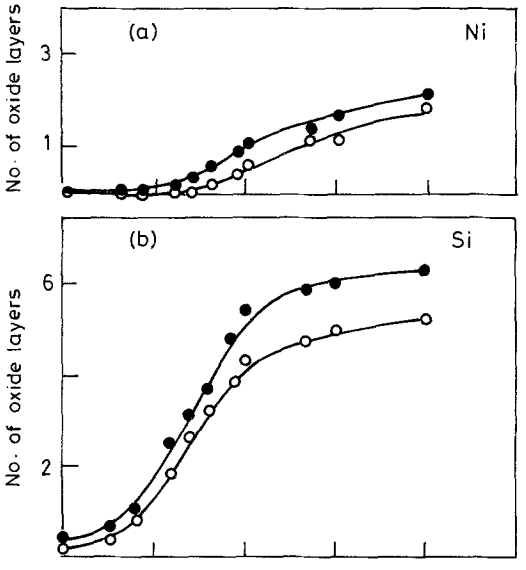

Figure 8 Number of oxide layers of Ni, Si and B formed in the surface oxidation of $Ni_{76}Si_{12}B_{12}$: •, metallic glass; ○, crystallized sample.

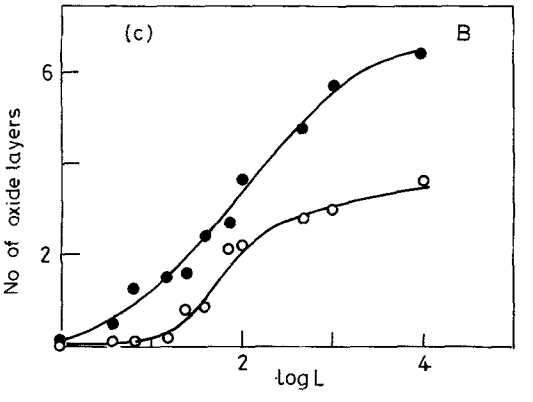

the crystalline state, contributing to the differences in the oxygen uptake with the amorphous sample. The number of oxide layers of nickel, boron, and silicon in the metallic glass and crystallized sample is plotted as a function of oxygen exposure in Fig. 8. We clearly see that the metalloid elements, boron and silicon, form a greater number of oxide layers in the metallic glass than in the crystallized sample, but the difference is not as appreciable in the case of nickel. This behaviour is somewhat different from that found in the $Fe_{40}Ni_{38}Mo_4B_{18}$ alloy, where the rates of oxidation of iron and nickel were less in the metallic glass as compared to the crystallized sample.

4. Conclusion

Surface oxidation of the metallic glasses and their crystallized sample depends to a large extent on the presence of the metalloid elements boron and silicon. One of the alloys, $Fe_{40}Ni_{38}Mo_4B_{18}$, offers a highly reactive surface for initial oxidation in the amorphous state, a possible protection mechanism against further oxidation. It is possible that the protection mechanism against the oxidation of metals such as iron and nickel by the metalloid elements may not be unique to the metallic glass alone but is related to the chemical composition.

Acknowledgement

The authors thank the Department of Science and Technology, Government of India and the Indian National Science Academy for support of this research.

References

1. S. EVANS, E. L. EVANS, D. E. PARRY, M. J. TRICKER, M. J. WALTERS and J. M. THOMAS, *Faraday Disc. Chem. Soc.* **58** (1974) 97.
2. C. N. R. RAO and M. S. HEDGE, in "Preparation and Characterization of Materials", edited by J. M. Honig and C. N. R. Rao (Academic Press, New York, 1981) p. 161.
3. A. SRINIVASAN, K. JAGANNATHAN and M. S. HEDGE, *Ind. J. Chem.* **18A** (1979) 463.
4. C. SURYANARAYANA, "Rapidly Quenched Metals" (Plenum, New York, 1980).
5. K. ASAMI, K. HASIMOTO, T. MASUMOTO and S. SHIMODAIRA, *Corrosion Sci.* **16** (1976) 909.
6. K. HASIMOTO, M. NAKA, K. ASAMI and T. MASUMOTO, *Corrosion Eng.* **27** (1978) 279.
7. C. N. R. RAO, D. D. SARMA and M. S. HEDGE, *Proc. Roy. Soc.* **A370** (1980) 269.
8. D. D. SARMA, M. S. HEDGE and C. N. R. RAO, *J. Chem. Soc. Faraday Trans II* **77** (1981) 1509.
9. F. P. FEHLNER and N. F. MOTT, "Oxidation of Metals" Vol. 2 (Plenum Press, New York, 1970) p. 59.
10. M. J. BRATHWAITE, R. W. JOYNER and M. W. ROBERTS, *Disc. Faraday Soc.* **60** (1975) 89.
11. P. SEN, M. S. HEDGE and C. N. R. RAO, *Appl. Surf. Sci.* **10** (1982) 63.
12. C. C. LO and H. G. TOMPKINS, *J. Appl. Phys.* **47** (1975) 3496.
13. L. LEY and J. D. RILEY, in "Proceedings of the 7th International Vacuum Congress", Vienna, March, 1977, Vol. 3, edited by R. Dobrozemsky, F. Rüdenauer, F. P. Viehböck and A. Breth, p. 2301.

Received 18 March
and accepted 24 June 1982